Final Report - SCEC 25063

Experimental Investigation of Coseismic Fault Re-strengthening

Xiaofeng Chen, Oklahoma State University

1. Introduction

Tectonic stress accumulation and release govern earthquake cycles. During long interseismic periods, tectonic stress builds up as faults remain locked, whereas this accumulated stress is released coseismically during earthquakes. Consequently, research has primarily focused on coseismic stress drop, or dynamic fault weakening, because of its direct relevance to earthquake initiation. Laboratory rock friction experiments have widely documented dynamic fault weakening at seismic slip velocities (e.g., Di Toro et al., 2011), and stick–slip instabilities that mimic earthquake cycles are understood to arise from the critical stiffness criterion (e.g., Leeman et al., 2016).

Notably, several experimental studies have reported coseismic dynamic restrengthening as slip velocity decreases toward arrest. Examples include high-speed velocity- and energy-controlled rotary shear experiments (e.g., Goldsby & Tullis, 2011; Chang et al., 2012; Proctor et al., 2014) and recent high-speed double-direct shear (DDS) experiments (Chen et al., 2025). This coseismic restrengthening exhibits a clear friction–velocity dependence consistent with flash-weakening theory, characterized by increasing friction as slip velocity decreases (Chen et al., 2025).

In stick–slip experiments, macroscopic friction typically decreases monotonically during the coseismic phase, and the slope of shear force versus fault slip reflects the unloading stiffness of the loading system (e.g., Xu et al., 2018). However, our stick–slip experiments conducted under both double-direct shear (DDS) and rotary shear configurations reveal consistent evidence of coseismic restrengthening (Chen et al., 2020, 2025). To further investigate this behavior, I performed additional stick–slip friction experiments using the Texas A&M DDS apparatus on Westerly granite and Sioux quartzite faults. The resulting mechanical data were analyzed to characterize the coseismic restrengthening.

2. Materials and Methods

Westerly granite and Sioux quartzite were selected for the friction experiments. The double-direct shear (DDS) configuration consists of a central block (5" × 2" × 2") sandwiched between two side blocks (3" × 2" × 1"). Flat fault surfaces were prepared using an 80-grit grinding wheel. High-resolution data acquisition at 25 kHz was achieved using a LabVIEW-based FPGA platform. Detailed descriptions of the apparatus and experimental procedures are provided in Chen et al. (2025). In selected stick–slip runs, the pneumatic chamber depressurization rate was adjusted to vary the stress buildup rate. In total, 29 stick–slip experiments were conducted on Westerly granite and 22 on Sioux quartzite under normal stresses ranging from 3 to 24 MPa (Table 1), with peak slip velocities reaching up to 0.63 m/s and 0.58 m/s for granite and quartzite faults, respectively.

Table 1. Summary of stick-slip experiments performed.

Westerly granite				Sioux quartzite			
#	Run #	Normal stress	Loading rate	#	Run #	Normal stress	Loading rate
1	619	9 MPa	1 mm/s	1	650	3 MPa	vary speed
2	620	9 MPa	1 mm/s	2	651	3 MPa	vary speed
3	621	12 MPa	1 mm/s	3	652	6 MPa	vary speed
4	622	12 MPa	1 mm/s	4	653	6 MPa	vary speed
5	623	15 MPa	1 mm/s	5	654	9 MPa	vary speed
6	624	12 MPa	1 mm/s	6	655	9 MPa	vary speed
7	625	18 MPa	1 mm/s	7	656	12 MPa	vary speed
8	626	18 MPa	1 mm/s	8	657	12 MPa	vary speed
9	627	21 MPa	1 mm/s	9	658	15 MPa	vary speed
10	628	21 MPa	1 mm/s	10	659	15 MPa	vary speed
11	629	24 MPa	1 mm/s	11	660	18 MPa	vary speed
12	630	24 MPa	1 mm/s	12	661	18 MPa	vary speed
13	636	3 MPa	vary speed	13	662	21 MPa	vary speed
14	637	3 MPa	vary speed	14	663	21 MPa	vary speed
15	638	6 MPa	vary speed	15	683	12 MPa	1 mm/s
16	639	6 MPa	vary speed	16	684	24 MPa	1 mm/s
17	640	6 MPa	vary speed	17	685	24 MPa	1 mm/s
18	641	9 MPa	vary speed	18	686	21 MPa	1 mm/s
19	642	9 MPa	vary speed	19	687	18 MPa	1 mm/s
20	643	10 MPa	vary speed	20	688	15 MPa	1 mm/s
21	644	14 MPa	vary speed	21	689	12 MPa	1 mm/s
22	645	12 MPa	vary speed	22	690	9 MPa	1 mm/s
23	646	12 MPa	vary speed				
24	647	15 MPa	vary speed				
25	648	15 MPa	vary speed				
26	649	18 MPa	vary speed				
27	680	9 MPa	1 mm/s				
28	681	18 MPa	1 mm/s				
29	682	18 MPa	1 mm/s				

3. Experimental Results

Both granite and quartzite faults exhibited pronounced stick–slip behavior under the tested conditions. Most stick–slip events in both lithologies display several common characteristics consistent with previous experimental observations, including: (1) shear stress drop proportional to peak slip velocity (Fig. 1); (2) both shear stress drop and peak velocity increase with increasing normal stress (Fig. 1) and stick-slips disappear when normal stress is smaller than ~3 MPa ; (3) longer interseismic loading durations lead to greater stress drops and higher peak velocities; and (4) recurrence intervals increase with higher normal stress and lower interseismic loading rates.

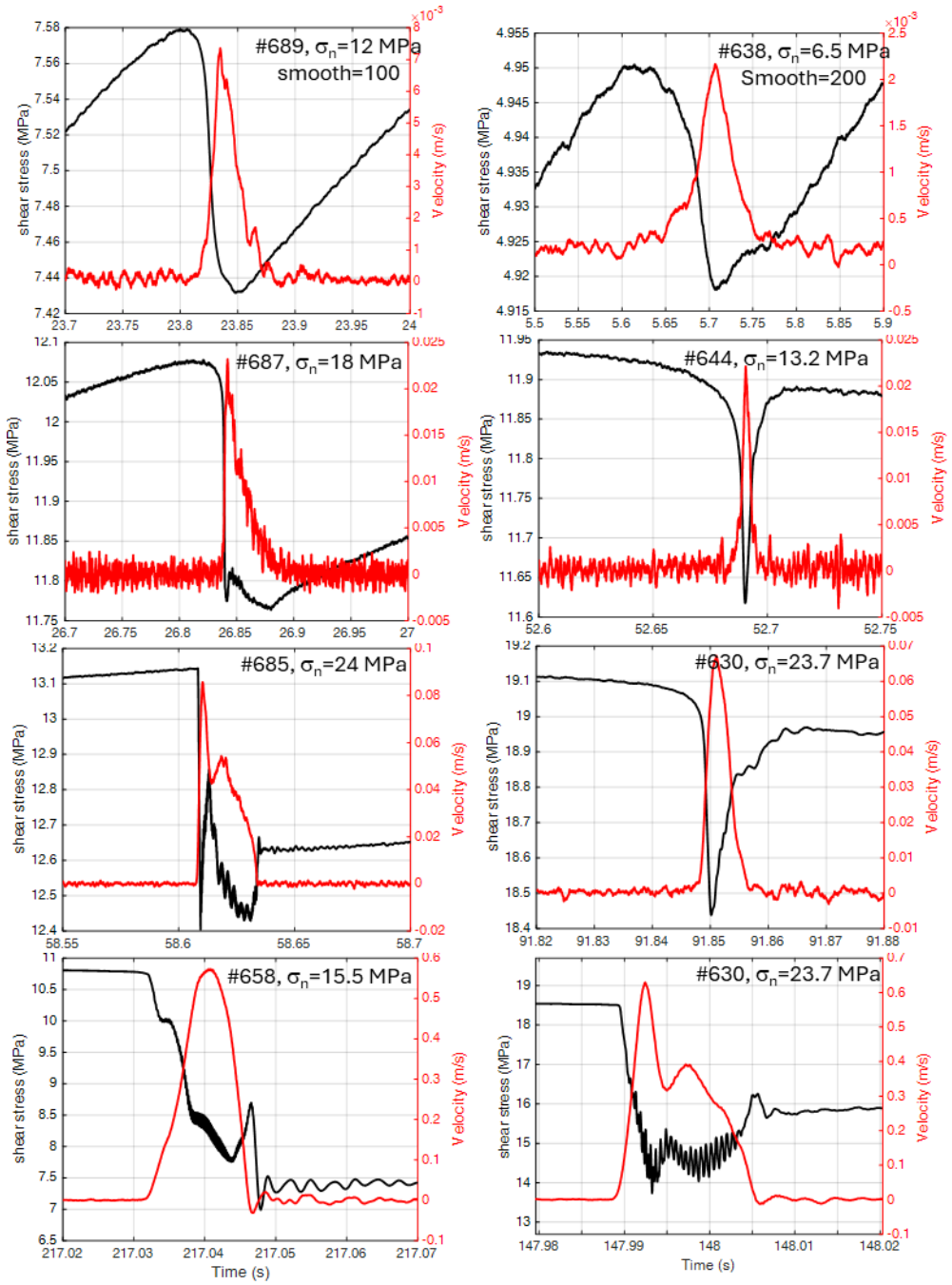

Figure 1. Shear stress and slip velocity histories of the Sioux quartzite (left column) and Westerly granite (right column). Velocity increases down each column, and each row shows similar velocity.

In contrast, clear distinctions between granite and quartzite faults are observed. Granite stick–slip events exhibit consistent coseismic weakening–strengthening behavior across all tested conditions (Fig. 1), with strengthening recovering approximately 50–80% of the initial stress drop (Fig. 2a). In comparison, quartzite stick–slip events show substantial variability in weakening–strengthening patterns (Fig. 1), with strengthening recovering only 5–70% of the initial dynamic weakening (Fig. 2a).

Similar contrasts are evident in slip velocity evolution. Granite stick–slip events generally display a symmetric velocity profile, characterized by comparable acceleration and deceleration rates at intermediate slip velocities up to ~0.1 m/s (Fig. 1). In contrast, quartzite stick–slip events exhibit a progressive transition in velocity evolution, ranging from near-symmetric profiles at low slip rates (~mm/s) to highly asymmetric profiles resembling a Yoffe-type function at intermediate slip rates (~cm/s), characterized by rapid acceleration to peak velocity followed by prolonged deceleration (Fig. 1). At higher, sub-seismic slip rates (>0.1 m/s), shear stress records commonly exhibit oscillatory behavior, representing a typical frictional response for siliceous faults (Chen et al., 2017). Under these conditions, velocity profiles may show multiple peaks or faster deceleration relative to acceleration.

Friction-peak velocity relations for both lithologies show a strong velocity-weakening correlation at velocities larger than ~0.1 m/s, consistent with the famous flash-weakening model prediction, whereas strong scatter occurs at lower velocities of less than 0.1 m/s (Fig. 2b). Notably, the granite fault exhibits a higher friction coefficient (~0.1 larger) than the quartzite fault.

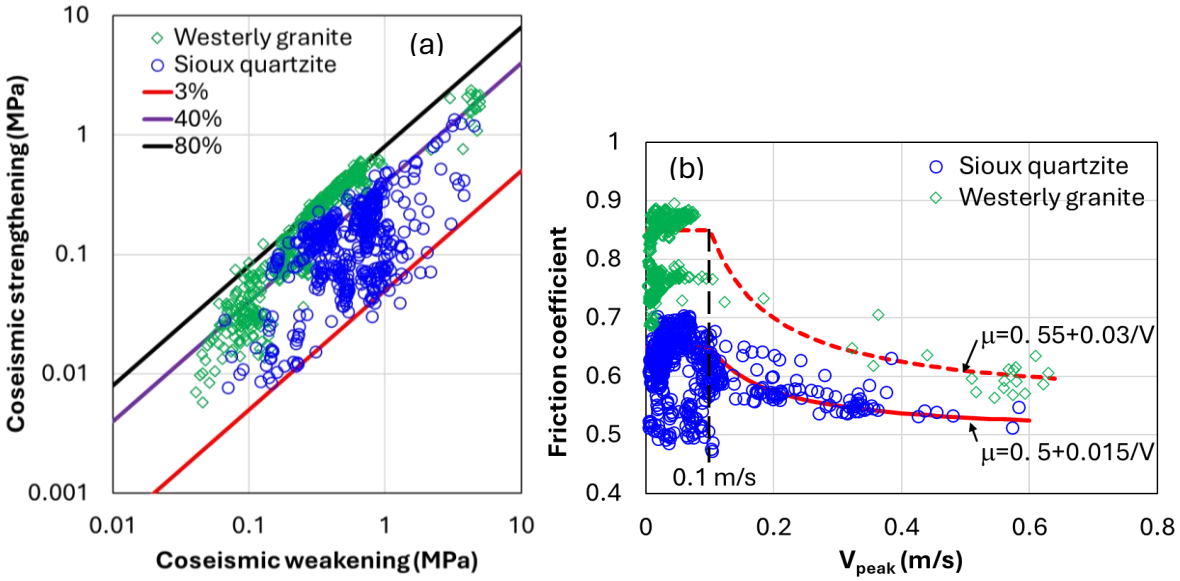

Figure 2. (a) Coseismic shear stress recovery versus maximum dynamic weakening during stick–slip events. Westerly granite shows a narrow recovery range of ~50–80%, whereas Sioux quartzite exhibits a broader range of ~5–70%. (b) Friction coefficient at peak slip velocity plotted against peak velocity for quartzite (blue circles) and granite (green diamonds). Both lithologies display strong velocity-dependent friction, with greater scatter at velocities <0.1 m/s and pronounced velocity weakening at >0.1 m/s. Granite consistently exhibits higher friction coefficients than quartzite. Best-fit relationships and corresponding equations are shown for each lithology.

4. Discussion

Within individual experiments, slight variations are observed between early and later stick–slip events, particularly at low normal stresses near the stability boundary of stick–slip instability. This behavior suggests an evolutionary effect influenced by cumulative slip history. Additional variability

is also evident between experiments conducted under similar loading conditions, as reflected by the scatter in the friction–velocity relationship (Fig. 2) and in the coseismic weakening–strengthening trends (Fig. 3). These variations highlight the inherent complexity of rock friction processes and indicate that factors beyond normal stress and loading rate influence frictional behavior. Such factors may include fault surface roughness, progressive microstructural evolution within the fault zone, and variations in dynamic rupture nucleation and propagation with cumulative slip and time.

We also observe a strong correlation between total coseismic stress drop (i.e., net dynamic weakening after restrengthening) and total coseismic slip. This relationship suggests that intermediate processes, such as dynamic weakening and restrengthening, do not significantly affect the initial and final stress states of the coseismic phase, consistent with the approximately constant unloading stiffness commonly observed in stick–slip experiments.

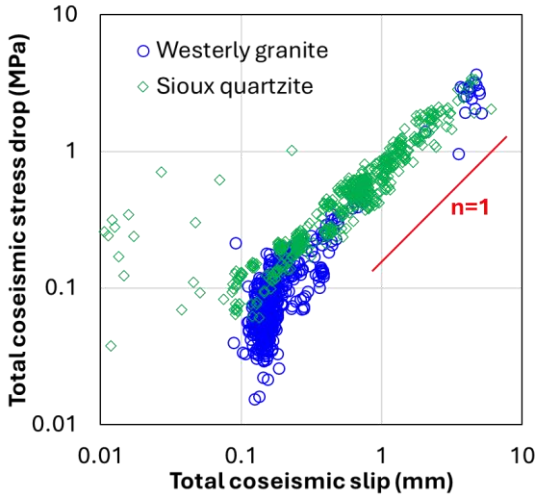

Figure 3. Total coseismic stress drop scales linearly with total coseismic slip for both granite and quartzite, despite minor scatter in the data at the low stress-drop end.

These experiments also demonstrate the importance of high sampling rates in stick–slip studies, as improved temporal resolution captures rapid stress and slip-velocity transients that may be unresolved at lower acquisition rates (Chen et al., 2020). In addition, increasing the resolution of stress and displacement measurements is essential, either through improved signal filtering or by employing higher-sensitivity sensors. Such enhancements are particularly critical for investigating stick–slip events with very small stress drops and displacements, including slow-slip phenomena.

5. References

Chang, J. C., Lockner, D. A., & Reches, Z. (2012). Rapid acceleration leads to rapid weakening in earthquake-like laboratory experiments. *science*, *338*(6103), 101-105.

Chen, X., Carpenter, B. M., & Reches, Z. E. (2020). Asperity failure control of stick–slip along brittle faults. *Pure and Applied Geophysics*, *177*(7), 3225-3242.

Chen, X., Elwood Madden, A. S., & Reches, Z. E. (2017). Friction evolution of granitic faults: heating controlled transition from powder lubrication to frictional melt. *Journal of Geophysical Research: Solid Earth*, *122*(11), 9275-9289.

Chen, X., Saber, O., & Chester, F. M. (2025). Velocity dependence of dynamic rock friction modulated by dynamic rupture in high-speed friction and stick-slip tests. *Journal of Geophysical Research: Solid Earth*, *130*(3), e2024JB030402.

Di Toro, G., Han, R., Hirose, T., De Paola, N., Nielsen, S., Mizoguchi, K., ... & Shimamoto, T. (2011). Fault lubrication during earthquakes. *Nature*, *471*(7339), 494-498.

Goldsby, D. L., & Tullis, T. E. (2011). Flash heating leads to low frictional strength of crustal rocks at earthquake slip rates. *Science*, *334*(6053), 216-218.

Leeman, J. R., Saffer, D. M., Scuderi, M. M., & Marone, C. (2016). Laboratory observations of slow earthquakes and the spectrum of tectonic fault slip modes. *Nature communications*, *7*(1), 11104.

Proctor, B. P., Mitchell, T. M., Hirth, G., Goldsby, D., Zorzi, F., Platt, J. D., & Di Toro, G. (2014). Dynamic weakening of serpentinite gouges and bare surfaces at seismic slip rates. *Journal of Geophysical Research: Solid Earth*, *119*(11), 8107-8131.

Xu, S., Fukuyama, E., Yamashita, F., Mizoguchi, K., Takizawa, S., & Kawakata, H. (2018). Strain rate effect on fault slip and rupture evolution: Insight from meter-scale rock friction experiments. *Tectonophysics*, *733*, 209-231.